

# DIFFUSE PIONIC GAMMA-RAY EMISSION FROM LARGE-SCALE STRUCTURES IN THE *FERMI* ERA

A. Dobardžić

*Department of Astronomy, Faculty of Mathematics, University of Belgrade, Studentski trg  
16, 11000 Belgrade, Serbia*

aleksandra@matf.bg.ac.rs

and

T. Prodanović

*Department of Physics, University of Novi Sad, Trg Dositeja Obradovića 4, 21000 Novi  
Sad, Serbia*

prodanvc@df.uns.ac.rs

## ABSTRACT

For more than a decade now the complete origin of the diffuse gamma-ray emission background (EGRB) has been unknown. Major components like unresolved star-forming galaxies (making  $\lesssim 50\%$  of the EGRB) and blazars ( $\lesssim 23\%$ ), have failed to explain the entire background observed by *Fermi*. Another, though subdominant, contribution is expected to come from the process of large-scale structure formation. The growth of structures is accompanied by accretion and merger shocks, which would, with at least some magnetic field present, give rise to a population of structure-formation cosmic rays (SFCRs). Though expected, this cosmic-ray population is still hypothetical and only very weak limits have been placed to their contribution to the EGRB. The most promising insight into SFCRs was expected to come from *Fermi*-LAT observations of clusters of galaxies, however, only upper limits and no detection have been placed. Here, we build a model of gamma-ray emission from large-scale accretion shocks implementing a source evolution calibrated with the *Fermi*-LAT cluster observation limits. Though our limits to the SFCR gamma-ray emission are weak (above the observed EGRB) in some case, in others, some of our models can provide a good fit to the observed EGRB. More importantly, we show that these large-scale shocks could still give an important contribution to the EGRB, especially at high energies. Future detections of cluster gamma-ray emission would help place tighter constraints on our models and give us a better insight into large-scale shocks forming around them.

*Subject headings:* cosmic rays – diffuse radiation – gamma rays: diffuse background – gamma rays: galaxies: clusters – large-scale structure of universe

## 1. INTRODUCTION

The extragalactic gamma-ray background (EGRB) was first detected by the *OSO-3* satellite (Kraushaar et al. 1972), confirmed by the *SAS-2* satellite (Fichtel et al. 1978; Thompson & Fichtel 1982), which was later succeeded by the *EGRET* (Strong et al. 2000), and has most recently been measured by the *Fermi*-LAT (Abdo et al. 2010) to unprecedented precision. In the search for the origin of the EGRB, multiple classes of sources were considered. Unresolved normal galaxies were found to be dominant contributors to the EGRB (Fields et al. 2010; Lacki et al. 2012). Other sources like blazars (Stecker & Salamon 1996; Narumoto & Totani 2007; Dermer 2007; Inoue & Totani 2009; Singal et al. 2012), pulsars (Higdon & Lingefelter 1976; Harding & Stecker 1981; Faucher-Giguère & Loeb 2010), dark matter annihilations (Scott et al. 2010; Abdo et al. 2010b), or secondary gamma-ray cascades (Murase et al. 2012; Inoue & Ioka 2012) were also considered. Even before *Fermi* era, Padovani et al. (1993) considered gamma-ray emission from cores of radio galaxies as a contributor to the EGRB for energies  $> 100$  MeV based on *Compton Gamma Ray Observatory* data. More recently, the contribution of radio galaxies using *Fermi* observations were considered in Inoue (2011). In most cases, none of these nor their combinations, managed to explain the entire background, though in a few models, some parameters can result in gamma-ray emission above the observed values. Analysis of the anisotropies in the EGRB (Ackermann et al. 2012a) and cross-correlations with source catalogs (Xia et al. 2011) can be used to constrain and discriminate between contributions of these unresolved sources. In terms of the guaranteed sources (Pavlidou & Fields 2002), *Fermi* observations revealed that the dominant emission mechanism is through cosmic-ray interaction with the gas in the interstellar medium (ISM), which produces neutral pions  $\pi^0$  which then decay into gamma rays  $p_{\text{cr}} + p_{\text{ism}} \rightarrow \pi^0 \rightarrow \gamma + \gamma$  (Stecker 1970, 1971). This process, where cosmic rays are accelerated in supernova remnants, is the dominant process responsible for the gamma-ray emission of observed star-forming galaxies (Strong et al. 1976; Pavlidou & Fields 2002; Prodanović & Fields 2006; Makiya et al. 2011) and contributes to the EGRB via unresolved star-forming galaxies. An accompanying leptonic component, namely inverse-Compton emission, was also analyzed, however it turned out to be subdominant to the hadronic component in star-forming galaxies contributing to the EGRB (Chakraborty & Fields 2012). Though normal galaxies are the most natural source of pionic gamma-ray emission because of their ongoing star-formation process that is constantly injecting cosmic rays into the ISM, quiescent galaxies rich in gas where cosmic rays are injected from Type Ia supernova events were

also analyzed and were found to be potentially important contributors to the EGRB in some cases (Lien & Fields 2012).

However, as cosmic rays are accelerated anywhere where shocks and magnetic fields are present, other cosmic-ray populations accelerated at different sites might also contribute to the observed EGRB. One such population are the cosmic rays accelerated during large-scale structure formation (SFCRs; Loeb & Waxman 2000; Furlanetto & Loeb 2004; Miniati et al. 2000), however, they are still hypothetical and yet to be observed. Good sites for observing potential gamma-ray emission from SFCRs are the nearby galaxy clusters (Völk et al. 1996; Berezhinsky et al. 1997; Enßlin et al. 1997; Colafrancesco & Blasi 1998; Kushnir & Waxman 2009; Pinzke & Pfrommer 2010), however observations have only placed upper limits so far by *Fermi* (Ackermann et al. 2010), and thus SFCRs remain undetected and their contribution to the EGRB remains unknown, with only weak limits placed (Miniati 2003; Prodanović & Fields 2004, 2005; Kuo et al. 2005). The search for emission from nearby galaxy clusters was also performed at TeV energies by telescopes like MAGIC (Aleksić et al. 2010), *H.E.S.S.* (Aharonian et al. 2009a,b), CANGAROO-III (Kiuchi et al. 2009), HEGRA (Aharonian et al. 2006), and Whipple telescope (Perkins et al. 2006), but again only upper limits have been reported. SFCRs should also be detectable with radio observations, since some merging galaxy clusters were already detected in radio waves (Brown & Rudnick 2011; van Weeren et al. 2011; Macario et al. 2011). Although cosmic rays that arise from processes responsible for growth of structures are yet to be detected, using in concert observations and limits at different energies will be important in revealing their signatures.

Nonetheless, given the importance of disentangling the origin of the EGRB and identifying its dominant components, in this work we build an improved and more detailed model of SFCR contribution to the EGRB. Since the history of this cosmic-ray population is unknown, as its tracer, we implement a semi-analytical source evolution of accretion shocks (Prodanović & Fields 2006). Another unknown required to make a prediction of their collective emission contributing to the EGRB is the gamma-ray flux expected from a single, average, large-scale shock. Though the cosmological shocks vary in scale and type (merger, accretion, filament), in our model, we will assume that accretion shocks around galaxy clusters are the dominant type of large-scale shocks, which allows us then to use cluster gamma-ray detection limits placed by *Fermi*. A similar approach was used in Kuo et al. (2005) to obtain the contribution of galactic clusters to the EGRB observed by *EGRET* but with a simpler source evolution. We note that only the pionic gamma-ray emission from SFCRs will be analyzed since it has been shown to be dominant over the inverse-Compton emission (Chakraborty & Fields 2012; Pinzke & Pfrommer 2010).

## 2. FORMALISM

The differential gamma-ray intensity  $dI_E/d\Omega$  ( $\text{cm}^{-2}\text{s}^{-1}\text{GeV}^{-1}\text{sr}^{-1}$ ) is an observable quantity that describes the EGRB. Following Pavlidou & Fields (2002, hereafter PF02) and Prodanović & Fields (2004) the differential gamma-ray intensity coming from SFCRs is

$$\frac{dI_E}{d\Omega} = \frac{c}{4\pi H_0} \int \frac{\dot{n}_{\gamma,\text{com}}[z, (1+z)E]}{\sqrt{\Omega_\Lambda + \Omega_m(1+z)^3}} dz, \quad (1)$$

where  $H_0$  is the present value of the Hubble parameter and  $z$  is the redshift of the source. Matter and vacuum energy density parameters are given as  $\Omega_m$  and  $\Omega_\Lambda$ , respectively. The differential co-moving gamma-ray emissivity density is  $\dot{n}_{\gamma,\text{com}}$ . In the case of gamma-ray emission from normal galaxies, where emission comes from cosmic rays accelerated in supernova remnants,  $\dot{n}_{\gamma,\text{com}}$  is a function of the number density of galaxies and their individual emission. This can be related to cosmic star-formation rate  $\dot{\rho}_*(z)$  as  $\dot{n}_{\gamma,\text{com}} = L_\gamma n_{\text{gal}} \propto \dot{\rho}_*(z)$  (see Equation (4) of PF02). In the case of SFCRs where the sources are large-scale structure formation shocks, their gamma-ray emissivity density,  $\dot{n}_{\gamma,\text{com}}$ , can be expressed in terms of a similar quantity which we call the cosmic accretion rate,  $\dot{\rho}_{\text{sf}}(z) = \int d\mathcal{M} d\dot{\rho}_{\text{sf}}(z, \mathcal{M})/d\mathcal{M}$  (co-moving mass current density crossing the surfaces of shocks of all Mach numbers at a given cosmic epoch in units of  $M_\odot \text{yr}^{-1} \text{Mpc}^{-3}$ ). Analytical models of cosmic accretion shocks were constructed by Pavlidou & Fields (2006, hereafter PF06) using the double distribution formalism of Pavlidou & Fields (2005). In their work, PF06 analyze cosmic shocks that arise on different accretors (with Press–Schechter mass distribution), at different epochs, in environments of different local over- and underdensities. They calculate the power and mass current that enters into these shocks of various strengths and follow their evolution over redshift, taking into account the effect of the environment such as the preheating. Furthermore, PF06 demonstrate that their models are consistent with energetics of accreted matter that results from simulations. We will use the model of PF06 to implement the evolution of SFCR sources, for which we thus implicitly take only the cosmic accretion shocks. The gamma-ray emission resulting from a cosmic-ray population scales as a product of cosmic-ray flux and total mass of targets  $L_\gamma \propto \phi_{\text{cr}} M_{\text{gas}}$ . We note, however, that the underlying assumption for which this relation holds is that the gas and cosmic-ray distributions are homogeneous within a system. Though this is true for galactic diffuse gamma-ray emission, for the case of large structures such as galaxy cluster, where we expect to find this cosmic-ray population, this would be most valid for the peripheral regions (Keshet 2010; Murase et al. 2008). More precise modeling of expected gamma-ray emission of a given accretor would have to include a thermal gas profile of the intra-cluster medium (Pfrommer & Enßlin 2004), and a more valid assumption would be that cosmic rays trace thermal gas distribution, which would alter the above relation and include additional parameters. However, for the purpose of this work,

where cluster gamma-ray emission upper limits will be utilized to constrain the accretion shock contribution to the EGRB, the details of a specific emission of a single accretor are not important, but will be included in a more extensive follow up analysis.

In the case of the galactic cosmic rays, their flux can be taken to be proportional to the star-formation rate, while similarly, in the case of cosmic rays originating from accretion shocks, the cosmic-ray flux can be taken to be proportional to the mass accretion rate (mass current crossing the shock surface in units  $M_{\odot}\text{yr}^{-1}$ ) of shocks at some object and some epoch,  $J(z)$ . With that set, a gamma-ray luminosity from structure formation process at some redshift can be determined as

$$L_{\gamma}(z, E) = \frac{J(z)}{J_0(z_0)} \frac{M_{\text{gas}}(z)}{M_{\text{gas}}(z_0)} L_{\gamma,0}(E), \quad (2)$$

where  $E$  is photon energy in the accretor rest frame and  $M_{\text{gas}}(z)$  is gas mass contained in the accretor at a given cosmic epoch  $z$ , i.e., the mass of the intracluster gas.  $J_0$  is the accretion rate at  $z_0$  to which we normalize. The gamma-ray luminosity of the normalization cluster, taken as the cosmic average, is then  $L_{\gamma,0}$ . The implicit assumption in the above equation is that the ratio of accelerated to accreted particles is a constant. The emissivity density can thus be written as  $\dot{n}_{\gamma,\text{com}}(z, E) = L_{\gamma}n_c$ . Co-moving galaxy cluster number density,  $n_c$ , and cosmic accretion rate,  $\dot{\rho}_{\text{sf}}(z)$ , are connected via  $\dot{\rho}_{\text{sf}}(z) = J(z)n_c$ . This gives the relation

$$\dot{n}_{\gamma,\text{com}}(z, E) = L_{\gamma,0}[(1+z)E] \frac{\dot{\rho}_{\text{sf}}(z)}{J_0(z_0)} \frac{M_{\text{gas}}(z)}{M_{\text{gas}}(z_0)}. \quad (3)$$

Assuming that, on the onset of accretion when structure was virialized, there was some initial gas mass  $M_{\text{gas},0}$  defined with respect to the accreted gas as  $M_{\text{gas},0} = \epsilon M_{\text{gas,acc}}(z_0)$ , the above gas mass ratio can be written in terms of the accreted mass ratio as

$$\frac{M_{\text{gas}}(z)}{M_{\text{gas}}(z_0)} = \frac{\epsilon + M_{\text{gas,acc}}(z)/M_{\text{gas,acc}}(z_0)}{1 + \epsilon}, \quad (4)$$

where  $M_{\text{gas,acc}}(z)$  and  $M_{\text{gas,acc}}(z_0)$  are masses of gas accreted from the epoch of virialization up to the redshifts  $z$  and  $z_0$ , respectively. The ratio of the accreted masses is equal to the ratio of the cosmic accretion rates during those same epochs

$$\frac{M_{\text{gas,acc}}(z)}{M_{\text{gas,acc}}(z_0)} = \frac{\int_{z_{\text{vir}}}^z dz (dt/dz) \dot{\rho}_{\text{sf}}(z)}{\int_{z_{\text{vir}}}^{z_0} dz (dt/dz) \dot{\rho}_{\text{sf}}(z)}. \quad (5)$$

Finally, following PF02, Equations (1), (2), (3), (4) and (5) combine to give the SFCR gamma-ray intensity as

$$\frac{dI_E}{d\Omega} = \frac{c}{4\pi H_0 J_0(z_0)} \int_0^{z_{\text{vir}}} dz \frac{\dot{\rho}_{\text{sf}}(z) L_{\gamma,0} [(1+z)E]}{\sqrt{\Omega_{\Lambda} + \Omega_{\text{m}}(1+z)^3}}$$

$$\times \left[ \frac{\epsilon}{\epsilon + 1} + (\epsilon + 1)^{-1} \frac{\int_{z_{\text{vir}}}^z dz (dt/dz) \dot{\rho}_{\text{sf}}(z)}{\int_{z_{\text{vir}}}^{z_0} dz (dt/dz) \dot{\rho}_{\text{sf}}(z)} \right], \quad (6)$$

where our solutions depend on the initial gas fraction parameter  $\epsilon$ , and the assumed spectral index,  $\alpha_\gamma$ .

### 3. INPUT

#### 3.1. Cosmic Accretion Rate

For the total mass current density of gas entering into accretion shocks at a given epoch, which we call the cosmic accretion rate  $\dot{\rho}_{\text{sf}}$ , we use models constructed in PF06. These models present an analytical description of the energetics of the population of cosmic accretion shocks. We utilize their derived mass current distribution among different shock Mach numbers and their evolution with cosmic time, as a tracer of structure formation shock history, and thus a tracer of SFCR history. We note however, that the results of PF06 that we use as cosmic accretion rate,  $\dot{\rho}_{\text{sf}}$ , reflect the evolution of a distribution of shock strength at each redshift, while in our work we assume that most emission comes from typical objects representative of the cosmic mean, with a single shock strength at each redshift.

Three models are separately analyzed in PF06. The simplest assumes that all objects are embedded in an environment well represented by the background universe. This model is based on the Press–Schechter formalism and will be labeled as Model 1 in our results. The second model of PF06 includes variations in the local matter density and temperature in the region around the accretor that are imprinted in the primordial density field and will be labeled as Model 2. The third, most realistic model, also includes filament preheating and compression. This model will be labeled as Model 3 in our results. The latter two models that include environmental effects are based on a double distribution which describes how the number density of collapsed and virialized dark matter objects is distributed among different masses and among different local density contrasts with respect to the cosmic mean density (Pavlidou & Fields 2005).

Since galactic cosmic rays are accelerated in supernova remnants, and star-formation rate reflects on the supernova rate, the cosmic star formation rate, which reflects the evolution of the star formation rate, can then be taken to reflect the evolution of galactic cosmic-ray sources. In a similar manner, if we assume that SFCRs are accelerated in accretion shocks, and that the integrated (over all accretion shocks of all Mach numbers) mass current density derived in PF06 models reflects the evolution of accretion shocks, then we can take that integrated mass current density reflects the evolution of SFCR source, i.e., take it as the

cosmic accretion rate,  $\dot{\rho}_{\text{sf}}$ .

### 3.2. Gamma-Ray Spectra

For the shape of the pionic gamma-ray spectrum  $\Gamma_{\gamma,\pi^0}(E)$ , we used the semi-analytical formula derived by Pfrommer & Enßlin (2003) as a representation of Dermer’s model (Dermer 1986). The spectrum in logarithmic space is symmetrical around half the pion rest mass,  $m_{\pi^0}$ , with the slope of the spectrum at high-energy end reflecting the spectral index  $\alpha_\gamma$  of cosmic rays, which we will leave as a free parameter in our model.

Even though large hopes were placed on *Fermi*-LAT when it comes to detection of galaxy clusters in gamma rays (Pinzke & Pfrommer 2010), no detections have been made yet. During the 18 months of *Fermi*-LAT observations, 33 clusters of galaxies were investigated and only upper limits have been reported (Ackermann et al. 2010). Still, one can use the reported upper limits to set the normalization of the SFCR component of the EGRB, which itself is then the upper limit. We choose to normalize to the Coma cluster as a typical cluster and thus use its *Fermi*-LAT upper limit, as well as other corresponding parameters entering Equation (6) such as the Coma redshift  $z_0 = 0.0232$  (Chen et al. 2007) and  $z_{\text{vir}} = 1.5$  (Brodwin et al. 2011) for its virialization. To determine  $L_{\gamma,0}$  we again assume a Pfrommer & Enßlin (2003) gamma-ray spectral shape  $\Gamma_{\gamma,\pi^0}(E)$ , the virial mass of Coma cluster  $M_{500} = 9.95 \times 10^{14} M_\odot$  (Chen et al. 2007; assumed to be the total mass of Coma cluster  $M_{\text{tot}}$ ), and the virial radius  $r_{500} = 1.86$  Mpc (Chen et al. 2007) which is defined as the radius at which the interior mass density equals  $500\rho_c$ , where  $\rho_c$  is the critical density at the redshift of the cluster. For the gas mass  $M_{\text{gas}}$  of Coma cluster, we use the value  $M_{\text{gas},500} = 19 \times 10^{13} M_\odot$  (Chen et al. 2007). With that set, and adopting the *Fermi* detection limit of Coma as actual detection with gamma-ray flux of  $F_{\gamma,0} = 4.58 \times 10^{-9}$  photon  $\text{cm}^{-2} \text{s}^{-1}$  (Ackermann et al. 2010) integrated over the energy range  $0.2 - 100$  GeV, the normalization of the luminosity spectrum of Coma can be derived by requiring that  $F_{\gamma,0} = \int dE L_{\gamma,0}(E)/4(1+z)d_c(z)^2\pi = C \int dE \Gamma_{\gamma,\pi^0}(E)/4(1+z)d_c(z)^2\pi$  where again  $\Gamma_{\gamma,\pi^0}(E)$  is the shape of pionic spectrum,  $C$  is the spectrum normalization constant and  $d_c(z) = 97$  Mpc is the co-moving distance of the cluster standardly defined as  $d_c(z) = (c/H_0) \int_0^z dz'/\sqrt{\Omega_M(1+z)^3 + \Omega_\Lambda}$ . Hence, the cluster luminosity is found to be  $L_{\gamma,0}(E) = 5.85 \times 10^{47} \Gamma_{\gamma,\pi^0}(E)$  photon  $\text{s}^{-1} \text{GeV}^{-1}$ .

Finally, one has to worry about how attenuation of gamma-ray photons by the extragalactic background light (EBL; Salamon & Stecker 1998; Stecker et al. 2006; Kneiske et al. 2004; Gilmore et al. 2009, 2012; Razzaque et al. 2009; Finke et al. 2010; Abramowski et al. 2013) will affect our results. Namely, high-energy gamma rays get attenuated by interact-

ing with the EBL which results in the electron–positron pair production. EBL consists of photons with wavelengths from ultraviolet to infrared, that come directly from stars or have been absorbed and reprocessed by dust in their host galaxies. *Fermi* observations of blazars and gamma-ray bursts have resulted in upper limits for EBL (Abdo et al. 2009, 2010c) and have detected an EBL redshift-dependent signature (Ackermann et al. 2012b). EBL attenuation was also recently measured in the spectra of the brightest blazars observed by *H.E.S.S.* (Abramowski et al. 2013). Since the electron–positron pair production cross section peaks at twice the electron mass, gamma-ray photons of energies  $\sim$  GeV are most likely to interact with UV background photons. Thus, models with high UV backgrounds will result in more suppression at high energies. The attenuation is redshift and energy-dependent and is significant at energies  $E > 100$  GeV. Although gamma-ray attenuation at higher redshifts is still highly uncertain, using the fiducial model for gamma-ray attenuation from Gilmore et al. (2012), we find that the modeled SFCR emission starts dropping after about  $E = 100$  GeV. This trend becomes even bigger after 1000 GeV, and after 10,000 GeV, no photons can reach us. This means that the attenuation of SFCR-produced gamma-ray photons by EBL might be visible when higher energy observations from *Fermi* become available.

One should also bare in mind that electron–positron pairs produced as a result of attenuation of gamma rays, could then inverse Compton scatter off the cosmic microwave background radiation and result in a secondary gamma-ray (cascade) emission component (Aharonian et al. 1994; Fan et al. 2004). This process results in a redistribution of gamma-ray photons from the high to low-energy end. Therefore, the cascade emission is especially important for hard gamma-ray sources whose emission extends to high energies. This type of emission is expected to contribute to the EGRB (Coppi & Aharonian 1997; Inoue & Totani 2009; Inoue & Ioka 2012; Murase et al. 2012) and should even start to dominate over the EBL-attenuated primary gamma-ray component at GeV – TeV energies. It was shown that the cascade emission can also depend on the strength of the intergalactic magnetic field (Yan et al. 2012; Venters & Pavlidou 2013). Namely, as the cascade particles get deflected in the magnetic field, this results in a “smearing out” the point source emission and could, with sufficiently strong magnetic fields, result in decreased brightness of a source to the point where it becomes unresolved, and its gamma-ray emission gets “merged” with the background. Since the intergalactic magnetic field is still unknown and only upper and lower limits exist (Neronov & Semikoz 2009), and since the cascade emission also depends on the spectrum of primary gamma rays which is a free parameter in our model, we at this point omit the calculation of cascade emission and present only primary gamma-ray emission produced by SFCR with attenuation included.



## 4. RESULTS

The contribution of SFCR interaction to EGRB was derived from Equation (6) based on the semi-analytical model of evolution of accretion shocks and the *Fermi*-LAT detection limit of the Coma cluster. The cosmological parameters used were  $\Omega_\Lambda = 0.7$ ,  $\Omega_m = 0.3$ , and  $H_0 = 71 \text{ km s}^{-1} \text{ Mpc}^{-1}$ . For our default case and results plotted in Figure 5 we adopt initial gas mass parameter,  $\epsilon = 0$ , and a spectral index typical of strong shocks,  $\alpha_\gamma = 2.1$  (we find the mean Mach numbers weighted by the accreted gas current for all three environment models of PF06 to all be consistent with strong shocks).

Our results are plotted in Figure 5 where we plot contributions of different components to the EGRB flux (data points) detected by *Fermi* (Abdo et al. 2010). The upper panel shows each component separately, while the bottom panel sums over components and gives the total predicted EGRB. The dash dotted line (red curve in the online version of the article) and dash dot dotted line (blue curve in the online version of the article) represent the contribution from star-forming galaxies in the two limiting cases of the model – luminosity evolution and density evolution respectively (Fields et al. 2010). The luminosity evolution scenario takes the redshift evolution of the galaxies in such a way so that luminosity of the galaxies was allowed to evolve while their co-moving number density was kept constant. Pure density evolution is the case where evolution lies in co-moving number density of normal galaxies while their luminosity is constant. The solid line is the blazar contribution (Abdo et al. 2010d). Contribution from SFCRs based on three different source models of PF06, and calibrated with Coma cluster detection limit, is represented by a long dashed (Model 1), short dashed (Model 2) and dotted curve (Model 3). The same line types relate to the same models on the bottom panel as well. The bottom panel shows the summed contribution from all components—blazars, star-forming galaxies, and SFCRs. Thick curves (and colored red in the online version of the article) correspond to the luminosity, while thin curves (and colored blue in on-line version of the article) correspond to the density evolution limiting case of the star-forming galaxy contribution to the EGRB as given in Fields et al. (2010). The EBL attenuation is also included, which impacts our results at  $E > 100 \text{ GeV}$ . What is apparent is that estimated diffuse gamma-radiation from SFCRs differs by more than one order of magnitude depending on which environment model was used; Model 1, with no environmental effects where collapsed structures accrete gas of uniform density and temperature, results in the lowest gamma-ray emission, while Model 3, where environmental effects were included (filament preheating) and virialized structures are located within preheated gas, results in the highest gamma radiation. This is a direct reflection of the difference in the integrated kinetic power of accretion shocks between these three models, as demonstrated in PF06.

In Figure 6, we demonstrate the sensitivity of our model with respect to the adopted

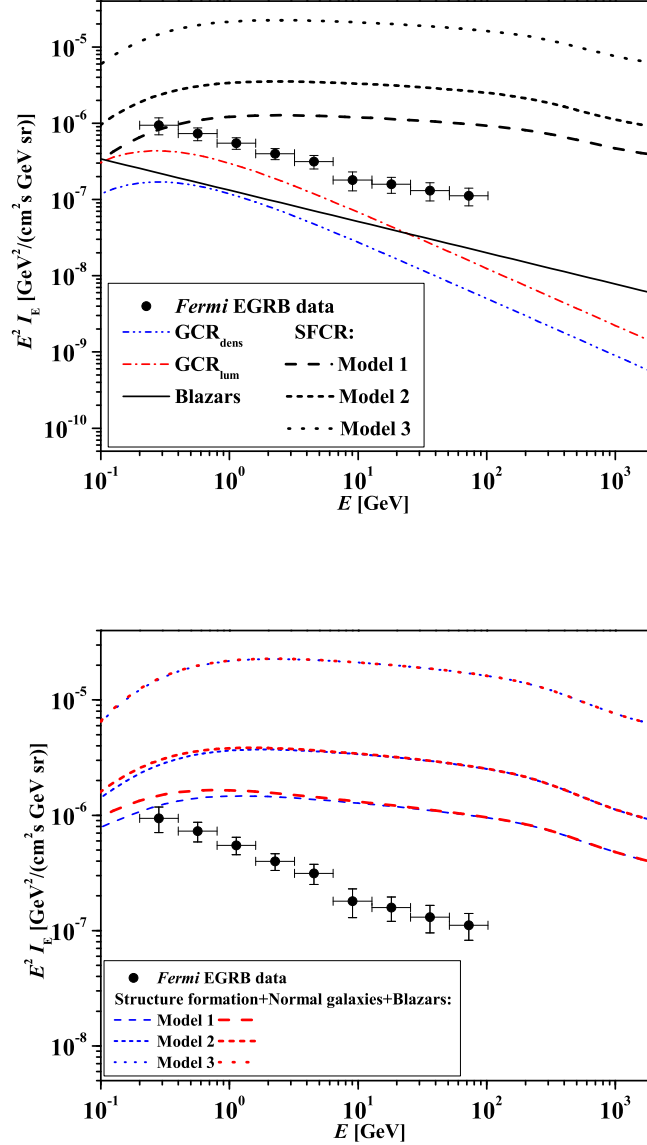


Fig. 1.— Contribution of different components to the EGRB (data points) observed by *Fermi* (Abdo et al. 2010). Top panel: all components shown separately – blazars (solid line), normal star-forming galaxies based on two limiting cases given in Fields et al. (2010; red dash dotted line represents luminosity evolution and blue dash dot dotted line represents density evolution), and structure-formation cosmic-ray contribution calculated in this work, normalized to the Coma cluster gamma-ray flux limit, with spectral index assumed to be  $\alpha_\gamma = 2.1$ , and initial gas mass parameter  $\epsilon = 0$ , for three different source models derived in Pavlidou & Fields (2006; long dashed, Model 1; short dashed, Model 2; dotted line, Model 3). Bottom panel: the combined contribution of all components where different curves reflect different normal galaxy emission models (thick red curves, luminosity evolution; thin blue curves, density evolution) and different structure-formation cosmic-ray emission models (three different line types correspond to the same models as on the top panel). (A color version of this figure is available in the online journal.)

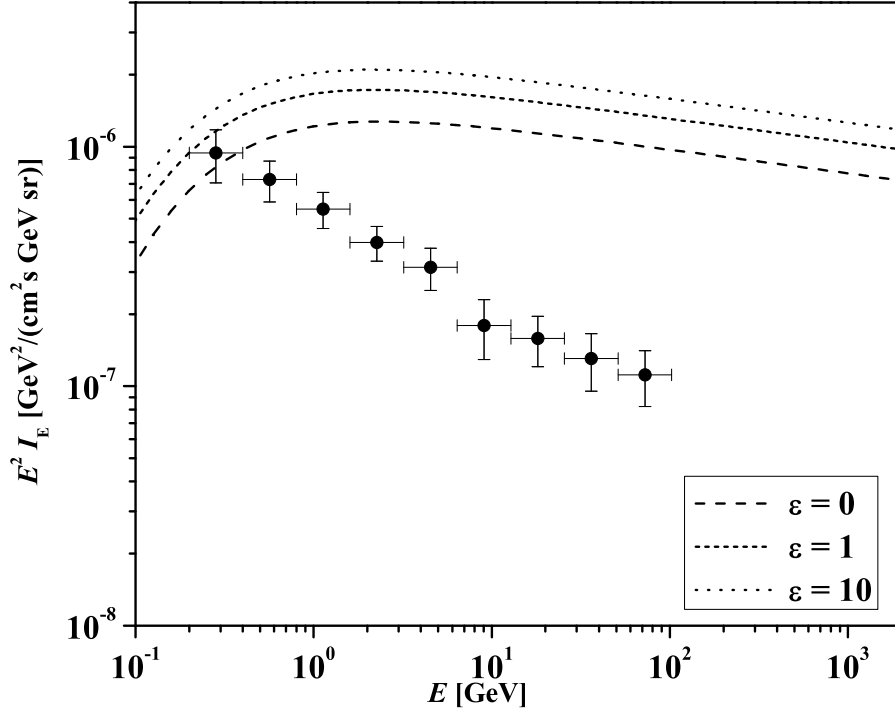


Fig. 2.— This plot shows the sensitivity of our model on the adopted initial gas mass fraction parameter  $\epsilon$ . For the purpose of demonstration, we plot the SFCR gamma-ray emission with spectral index  $\alpha_\gamma = 2.1$ , based on Model 1 of PF06, and derived adopting different initial gas mass fraction values,  $\epsilon = 0, 1, 10$ . The top most curve is approximately a factor of two higher than our fiducial case plotted in Figure 5. For all  $\epsilon > 10$ , all curves converge and are overlapping with the  $\epsilon = 10$  curve.

initial gas mass content of a cluster represented by the parameter  $\epsilon$ . We see that for the two most extreme cases, our fiducial case,  $\epsilon = 0$ , and our limiting case,  $\epsilon = 10$  (note that for  $\epsilon > 10$  the curves converge), the resulting curves differ by a factor of  $\sim 2$ . To be as conservative as possible, we thus keep  $\epsilon = 0$  as our fiducial value.

In Figure 3, we show how our results change with a different choice of the spectral index. The SFCR gamma-ray component with spectral indices ranging from 2–3 is plotted for different PF06 models: Model 1, top panel; Model 2, middle panel; and Model 3, bottom panel.

Our results for the fiducial case of strong shocks show that the observed EGRB is best matched with the SFCR component where source evolution is based on the most simple model with no environmental effects taken into account, Model 1 of PF06, while other models overshoot the observed data. However, given that we have normalized our models to the upper limit of the Coma cluster emission, this is the most generous estimate of the SFCR contribution to the EGRB. Once the cluster(s) has been detected, or if a detailed cluster emission model is implemented, our upper limits would become predictions, but could also accommodate Models 2 and 3 with softer emission.

## 5. DISCUSSION AND CONCLUSION

We have constructed a model of the collective gamma-ray emission arising from the large scale accretion shocks around virialized structures and estimated its contribution to the extragalactic gamma-ray background for various parameter values. Assuming that accretion shocks give rise to a new population of cosmic rays, the SFCRs, this would inevitably result in a gamma-ray flux which would contribute to the observed (but still unexplained!) EGRB at some level. Given that SFCRs are still a hypothetical population, with no direct observational evidence and no known source evolution, so far only very weak upper limits have been placed to their contribution to the EGRB.

Analytically modeling cluster formation and evolution, and including different sources of particle acceleration, Colafrancesco & Blasi (1998) have estimated the cluster contribution to the gamma-ray background to be  $\lesssim 1\%$  of the EGRB measured by *EGRET* (Strong et al. 2000), while numerical models estimate it to be of the order of  $\lesssim 10\%$  (Miniati 2002). However, the latest measurements by *Fermi* show the EGRB intensity above 100 MeV to be about a factor of 1.4 lower (Abdo et al. 2010) than previously estimated, thus making the SFCR contribution to the gamma-ray background correspondingly larger. This is especially important at higher energies where the *Fermi* measured EGRB is almost an order of mag-

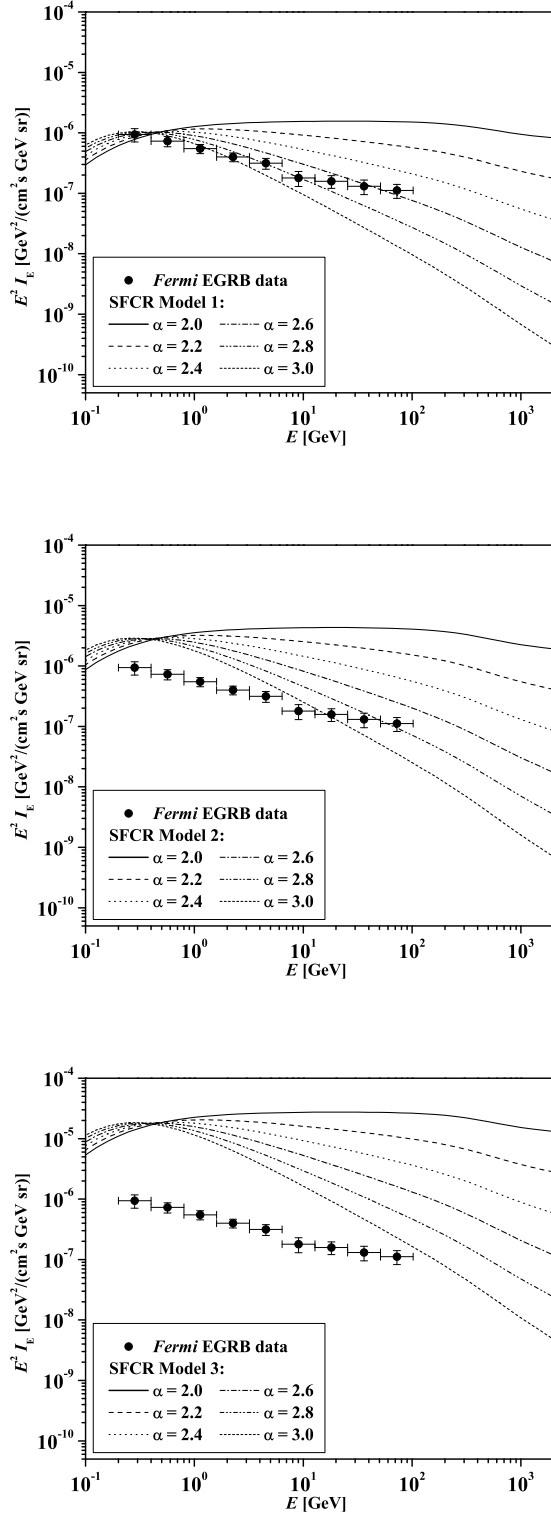


Fig. 3.— Contribution of structure-formation cosmic rays to the EGRB (data points) observed by *Fermi* (Abdo et al. 2010) for different choices of the cosmic-ray spectral index ranging from  $\alpha_\gamma = 2$  to  $\alpha_\gamma = 3$ , for Model 1 (top panel), Model 2 (middle panel) and Model 3 (bottom panel). The Coma cluster was again taken as the normalizing object with  $\epsilon = 0$ .

nitude lower than inferred from *EGRET*, e.g., making the Strong et al. (2000) estimate of the pionic SFCR component at the  $\sim 40\%$  level of the EGRB.

In this work, we have implemented source evolution based on the PF06 (Prodanović & Fields 2006) analytical model of cosmic accretion shocks around virialized structures within different environments, with spectral index of the source gamma-ray emission as a free parameter. The results of our analysis are, in some cases, consistent with previous estimates that this component is subdominant to all other EGRB sources (Miniati 2002; Colafrancesco & Blasi 1998; Kuo et al. 2005); however, we also show that there are scenarios where accretion shocks on clusters can have an important contribution to the EGRB.

To calibrate the resulting spectrum, we have used the unresolved source (point source) gamma-ray flux upper limits reported by *Fermi* for galaxy clusters (Ackermann et al. 2010), specifically the Coma cluster; thus, our results presented in this work are the upper limits. Moreover, by using these limits, our results are free of any assumption about the profile of the intracluster medium. Taking into account a spatial profile would give a stronger limit, but we leave that analysis for the follow up work.

Our results, for our fiducial case of strong accretions shocks normalized to the Coma cluster, are presented in Figure 5. We see that the contribution of cosmic rays, arising from accretion shocks, to the observed EGRB can be dominant, especially at energies  $> 10$  GeV compared to cosmic rays originating from star-forming galaxies. Moreover, depending on the assumptions, our discussed models go above the observed EGRB limits, allowing sufficient room for recalibration once clusters have been detected by gamma-ray observations, or when a detailed model of cluster emission is implemented. Thus, a positive cluster detection would not only make our upper limit model of SFCR contribution to the EGRB into a prediction, but would also serve, within our model, as a probe of the SFCR source evolution. For the specific case of the Coma cluster, such detection might be within reach, given that new predictions (Brunetti et al. 2012), which are at the same time successful in explaining the Coma cluster radio halo, fall just below the present *Fermi* limits. On the other hand, our limits to SFCR gamma-ray emission can also be used to discriminate between different models (Brunetti et al. 2012; Pinzke & Pfrommer 2010) of hadronic emission from the Coma cluster. Recently, Keshet et al. (2012) have reported a detection with VERITAS Cherenkov array of the gamma-ray ring around the Coma cluster. The reported signal is claimed to be synchrotron and inverse-Compton emission from relativistic electrons accelerated in large-scale shocks. Since the hadronic gamma-ray emission is thought to be subdominant in the reported signal, we cannot directly use this to calibrate our model; however, if confirmed, such detection would be important for constraining the population of SFCRs around clusters.

In terms of model dependence, our predicted limit is slightly sensitive to the choice

of the virialization redshift of the accretor. Normalizing to a galaxy cluster with a larger virialization redshift would result in a slightly higher collective gamma-ray emission and contribution to the EGRB. On the other hand, the choice of an environment model for the cosmic accretion rate  $\dot{\rho}_{\text{sf}}$  from PF06 can change the results by about one order of magnitude. The impact of a different choice of the environment in the source evolution model is best evident at the low-energy end of Figure 3. Using the simplest model (Model 1) presented in PF06, which was based only on the Press–Schechter distribution, where all objects accrete baryons of the uniform density and temperature, the resulting spectrum is lower than in the case of a more realistic model with density and temperature variations around the accretor. Even though it involves the most simplistic assumptions, we find that the choice of Model 1 for our source evolution, results in the SFCR gamma-ray component that best fits the observed EGRB. Our results are also very sensitive to the choice of the spectral index of gamma-ray emission of a typical source, which is best evident at the high energy end of Figure 3. This also results in variations by about an order of magnitude within a chosen environment model. When more data at the high energy end becomes available, this will be important in determining the typical environment and spectral index of a typical SFCR source.

Finally, our model is also strongly dependent on the choice of the galaxy cluster to which we normalize, which can change the resulting spectrum up to two orders of magnitude, depending on the cluster size, distance, mass, and its reported flux upper limit. Given the setup of our model, the normalizing cluster should be representative of the cosmic mean with respect to the cluster mass. On the other hand, given that no cluster was actually detected and that only upper limits are available, ideally, the normalizing cluster should also be the one with its limit closest to its pionic gamma-ray emission. We have considered several clusters as candidates for the normalizing cluster, and eventually chose the Coma cluster. Though Coma is a rich cluster, it has intermediate values of cluster size, mass, and flux upper limit, where its predicted pionic emission is at the level of its *Fermi* limit (Brunetti et al. 2012). Other considered clusters were not as suitable as Coma for various reasons. For instance, Perseus is a cluster slightly smaller than Coma but its predicted flux upper limit is large because *Fermi* sensitivity for this cluster is affected by foreground emission from the Galactic plane and other bright gamma-ray sources (Ackermann et al. 2010). Another considered candidate was the NGC5813 cluster, which is smaller than Coma with mass  $M_{500} = 4.3 \times 10^{13} M_{\odot}$  (Chen et al. 2007) and closer to the cosmic average. However, this cluster has a weaker *Fermi* limit, and thus, the resulting upper limits to the SFCRs contribution to the EGRB would be weaker by a factor of  $\approx 1.5$  than in the case of Coma. On the other hand, Fornax is a cluster with mass  $M_{500} = 1.24 \times 10^{14} M_{\odot}$  (Chen et al. 2007), which is around eight times smaller than  $M_{500}$  for Coma; however it is expected to be dominated by the dark matter

annihilation signal (Pinzke et al. 2011) and thus would not be a good choice for normalization of our model.

Even though our new constraints on the SFCR contribution to the EGRB are quite model-dependent and represent limits, the results indicate that there is still possible importance of this gamma-ray component which could have multiple implications. For instance, a concern was raised that SFCRs could potentially produce important quantities of lithium isotopes which would increase the severity of the lithium problem (Prodanović & Fields 2007; Suzuki & Inoue 2002). Since we have shown that the SFCR contribution to the EGRB can be important, corresponding lithium production (Fields & Prodanović 2005) could also be relevant. Similarly, neutrino fluxes accompanying this cosmic-ray population could also make an important contribution to the neutrino background arising from other sources like dark matter annihilations (Colafrancesco & Blasi 1998; Murase & Beacom 2012). Therefore, it is not only important to detect or build a careful model of accretion shock cluster emission, but to also let the sources evolve within a carefully treated environment, because this can greatly affect the resulting gamma-ray emission.

We are grateful to Vasiliki Pavlidou and Brian Fields for insightful discussions and comments and valuable help with data. We are also thankful to the anonymous Referee whose comments helped improve this paper. The work of AD is supported by the Ministry of Science of the Republic of Serbia under project number 176005 and the work of TP is supported in part by the Ministry of Science of the Republic of Serbia under project numbers 171002 and 176005.

## REFERENCES

- Abdo, A. A., Ackermann, M., Ajello, M. et al., 2010a, *PhRvL*, 104, 101101
- Abdo, A. A., Ackermann, M., Ajello, M. et al., 2010b, *JCAP*, 04, 014
- Abdo, A. A., Ackermann, M., Ajello, M., et al., 2010c, *ApJ*, 723, 1082
- Abdo, A. A., Ackermann, M., Ajello, M., et al., 2010d, *ApJ*, 720, 435
- Abdo, A. A., Ackermann, M., Arimoto, M., et al., 2009, *Sci*, 323, 1688
- Abramowski, A., Acero, F., Aharonian, F. (H.E.S.S. Collaboration), et al., 2013, *A&A*, 550, A4
- Ackermann, M., Ajello, M., Albert, A., et al., 2012a, *PhRvD*, 85, 083007



- Ackermann, M., Ajello, M., Allafort, A., et al., 2010, *ApJL*, 717, L71
- Ackermann, M., Ajello, M., Allafort, A., et al., 2012b, *Sci*, 338, 1190
- Aharonian, F., Akhperjanian, A. G., Anton, G., et al., 2009a, *A&A*, 495, 27
- Aharonian, F., Akhperjanian, A. G., Anton, G., et al., 2009b, *A&A*, 502, 437
- Aharonian, F., Akhperjanian, A., Beilicke, M., et al., 2006, *A&A*, 454, 775
- Aharonian, F. A., Coppi, P. S., & Voelk, H. J. 1994, *ApJL*, 423, L5
- Aleksić, J., Antonelli, L. A., Antoranz, P., et al., 2010, *ApJ*, 710, 634
- Berezinsky, V. S., Blasi, P., & Ptuskin., V. S. 1997, *ApJ*, 487, 529
- Brodwin, M., Stern, D., Vikhlinin, A., et al., 2011, *ApJ*, 732, 33
- Brown, S., & Rudnick, L. 2011, *MNRAS*, 412, 2
- Brunetti, G., Blasi, P., Reimer, O. et al., 2012, *MNRAS*, 426, 956
- Chakraborty, N., & Fields, B. D., 2012, *ApJ*, 773, 14
- Chen, Y., Reiprich, T. H., Böhringer, H., Ikebe, Y., & Zhang, Y. Y. 2007, *A&A*, 466, 805
- Colafrancesco, S., & Blasi, P. 1998, *APh*, 9, 227
- Coppi, P. S., & Aharonian, F. A. 1997, *ApJL*, 487, L9
- Dermer, C. D. 1986, *A&A*, 157, 223
- Dermer, C. D. 2007, in *AIP Conf. Proc.*, The First GLAST Symposium, Vol. 921 (Melville, NY: AIP; Steven Ritz, Peter Michelson and Charles A. Meegan), 122
- Enßlin, T. A., Bierman, P. L., Kronberg, P. P., & Wu, X. 1997, *ApJ*, 477, 560
- Fan, Y. Z., Dai, Z. G., & Wei, D. M. 2004, *A&A*, 415, 483
- Faucher-Giguère, C. A., & Loeb, A. 2010, *JCAP*, 01, 005
- Fichtel, C. E., Simpson, G. A., & Thompson, D. J. 1978, *ApJ*, 222, 833
- Fields, B. D., Pavlidou, V., & Prodanović, T. 2010, *ApJL*, 722, 199
- Fields, B. D., & Prodanović, T. 2005, *ApJ*, 623, 877

- Finke, J. D., Razzaque, S., & Dermer, C. D. 2010, *ApJ*, 712, 238
- Furlanetto, S. R., & Loeb, A. 2004, *ApJ*, 611, 642
- Gilmore, R. C., Madau, P., Primack, J. R., et al., 2009, *MNRAS*, 399, 1694
- Gilmore, R. C., Somerville, R. S., Primack, J. R., et al., 2012, *MNRAS*, 422, 3189
- Harding A. K., & Stecker F. W. 1981, *Natur*, 290, 316
- Higdon, J. C., & Lingenfelter, R. E. 1976, *ApJL*, 208, L107
- Inoue, Y. 2011, *ApJ*, 733, 66
- Inoue, Y., & Ioka, K. 2012, *PhRvD*, 86, 023003
- Inoue, Y., & Totani, T. 2009, *ApJ*, 702, 523
- Keshet, U. 2010, *arXiv:1011.0729*
- Keshet, U., Kushnir, D., Loeb, A., & Waxman, E. 2012, *arXiv:1210.1574*
- Kiuchi, R., Mori, M., Bicknell, G. V., et al., 2009, *ApJ*, 704, 240
- Kneiske, T. M. 2008, *ChJAS*, 8, 219
- Kneiske, T. M., Bretz, T., Mannheim, K. & Hartmann, D. H. 2004, *A&A*, 413, 807
- Kraushaar, W. L., Clark, G. W., Garmire, G. P. et al., 1972, *ApJ*, 177, 341
- Kuo, P.-H., Bowyer, S., & Hwang, C.-Y. 2005, *ApJ*, 618, 675
- Kushnir, D., & Waxman, E. 2009, *JCAP*, 08, 002
- Lacki, B. C., Horiuchi, S., & Beacom, J. F. 2012, *arXiv:1206.0772*
- Lien, A., & Fields, B. D. 2012, *ApJ*, 747, 120
- Loeb, A., & Waxman, E. 2000, *Natur*, 405, 156
- Macario, G., Markevitch, M., Giacintucci, S., et al., 2011, *ApJ*, 728, 82
- Makiya, R., Totani, T., & Kobayashi, M. A. R. 2011, *ApJ*, 728, 158
- Miniati, F. 2002, *MNRAS*, 337, 199
- Miniati, F. 2003, *MNRAS*, 342, 1009

- Miniati, F., Ryu, D., Kang, H., et al., 2000, *ApJ*, 542, 608
- Murase, K. & Beacom, J. F. 2012, *JCAP*, 02, 028
- Murase, K., Beacom, J. F., & Takami, H. 2012, *JCAP*, 08, 030
- Murase, K., Inoue, S., & Nagataki, S. 2008, *ApJL*, 689, L105
- Narumoto, T., & Totani, T. 2007, *Ap&SS*, 309, 73
- Neronov, A. & Semikoz, D. V. 2009, *PhRvD*, 80, 123012
- Padovani, P., Ghisellini, G., Fabian, A. C., & Celotti, A. 1993, *MNRAS*, 260, L21
- Pavlidou, V., & Fields, B. D. 2002, *ApJL*, 575, L5
- Pavlidou, V., & Fields, B. D. 2005, *PhRvD*, 71, 043510
- Pavlidou, V., & Fields, B. D. 2006, *ApJ*, 642, 734
- Perkins, J. S., Badran, H. M., Blaylock, G., et al., 2006, *ApJ*, 644, 148
- Pfrommer, C., & Enßlin, T. A. 2003, *A&A*, 407, 73
- Pfrommer, C., & Enßlin, T. A. 2004, *A&A*, 413, 17
- Pinzke, A., & Pfrommer, C. 2010, *MNRAS*, 409, 449
- Pinzke, A., Pfrommer, C., & Bergström, L. 2011, *PhRvD*, 84, 123509
- Prodanović, T., & Fields, B. D. 2004, *APh*, 21, 627
- Prodanović, T., & Fields, B. D. 2005, *SerAJ*, 170, 33
- Prodanović, T., & Fields, B. D. 2006, *ApjL*, 645, L125
- Prodanović, T., & Fields, B. D. 2007, *PhRvD*, 76, 083003
- Razzaque, S., Dermer, C. D., & Finke, J. D. 2009, *ApJ*, 697, 483
- Salamon, M. H., & Stecker, F. W. 1998, *ApJ*, 493, 547
- Scott, P., Conrad, J., Edsjo, J., et al., 2010, *JCAP*, 01, 031
- Singal, J., Petrosian, V., & Ajello, M. 2012, *ApJ*, 753, 45
- Stecker, F. W. 1970, *Ap&SS*, 6, 377

- Stecker, F. W. 1971, NASSP, 249, 499
- Stecker, F. W., Malkan, M. A. & Scully, S. T. 2006, ApJ, 648, 774
- Stecker, F. W., & Salamon, M. H. 1996, ApJ, 464, 600
- Strong, A. W., Moskalenko, I. V., & Reimer, O. 2000, ApJ, 537, 763
- Strong, A. W., Wolfendale, A. W., & Worrall, D. M. 1976, MNRAS, 175, 23P
- Suzuki, T. K., & Inoue, S. 2002, ApJ, 573, 168
- Thompson, D. J., & Fichtel, C. E. 1982, A&A, 109, 352
- van Weeren, R. J., Hoeft, M., Röttgering, H. J. A., et al., 2011, A&A, 528, 13
- Venters, T. & Pavlidou, V. 2013, MNRAS, 432, 3485
- Völk, H. J., Aharonian, F. A., & Breitschwerdt, D. 1996, SSRv , 75, 279
- Xia, J.-Q., Cuoco, A., Branchini, E., Fornasa, M., & Viel, M. 2011, MNRAS, 416, 2247
- Yan, D., Zeng, H., & Zhang, L. 2012, MNRAS, 422, 1779

**ERRATUM: "DIFFUSE PIONIC GAMMA-RAY EMISSION FROM  
LARGE-SCALE STRUCTURES IN THE *FERMI* ERA" (2014, ApJ, 782, 109)**

A. Dobardžić

*Department of Astronomy, Faculty of Mathematics, University of Belgrade, Studentski trg  
16, 11000 Belgrade, Serbia*

`aleksandra@matf.bg.ac.rs`

T. Prodanović

*Department of Physics, University of Novi Sad, Trg Dositeja Obradovića 4, 21000 Novi  
Sad, Serbia*

`prodanvc@df.uns.ac.rs`

The published version of this article contained a computational error in calculation of the mass accretion rate  $J_0$  (mass current crossing the shock surface in units of  $M_\odot\text{yr}^{-1}$ ) at redshift  $z_0$  of the galactic cluster to which we normalize our models of structure formation cosmic rays. The mass accretion rate  $J_0$  was calculated using Pavlidou & Fields (2006):

$$J_0(z_0) = 4\pi r_v^2(m)\Omega_b\rho_{c,0}(1+z_0)^3(1+\delta_s)\mathcal{M}c_{s,1}, \quad (7)$$

where  $\Omega_b = 0.04$  is the baryonic matter energy density parameter,  $\rho_{c,0}$  is the critical density at the present epoch,  $c_{s,1}$  is the adiabatic sound speed of the pre-shocked material,  $\delta_s$  is the overdensity in which the accretor is located,  $r_v$  is the virial radius of the accretor. Mach number of the accretion shock is  $\mathcal{M}$ . We chose to normalize to Coma cluster, so the correct value of the accretion rate for this cluster is  $J_0 = 417.86 M_\odot\text{yr}^{-1}$ . This value is an order of magnitude lower than the value used in the published version of the paper. This does not change our main conclusion that structure formation cosmic rays can make an important contribution to the extragalactic gamma-ray background, but it does change the parameter values of the best-fit model. All of our models now give an order of magnitude higher gamma-ray flux, which now puts a tighter constraints on the ones that are allowed by the data.

The observed extragalactic gamma-ray background is, as in the published version, best matched by the structure formation cosmic-ray component where source evolution is based on the most simple model with no environmental effects taken into account, Model 1 of Pavlidou & Fields (2006), while other models overshoot the observed data. In the Results

section of the published version we have adopted as our default case the spectrum where the initial gas mass parameter was taken to be  $\epsilon = 0$ , while the adopted spectral index was that of the strong shocks  $\alpha_\gamma = 2.1$ . Since our curves are now higher, even our simplest model is above the extragalactic gamma-ray background observed by the *Fermi* for strong shocks spectral indices  $\alpha_\gamma \approx 2$ . Our most probable scenario is now for the spectral index 2.7 (Model 1). This is close to Brunetti et al. (2012) where they found best-fit of the Coma spectrum to be derived using spectral index  $\approx 2.6$ . Although even in this case of the softer spectra, the model does overshoot the data at some energy ranges, we remind that our normalization was based on the Coma gamma-ray upper limit as reported by *Fermi*, and thus leaves room for downward correction once the detection is made or when a specific emission model is used.

We plot Figure 1 with the same parameters, just like in the published version of the paper, but with now corrected value of  $J_0$  (top panels). Here we also add the same plots of our best-fit scenario with spectral index 2.7 (bottom panels). Figure 1 shows contributions of structure formation cosmic rays, normal galaxies and blazars shown separately (left), as well as their summarizes contribution (right). We also correct Figure 2 from our published paper using our best-fit spectral index 2.7 instead of 2.1 which was used before. Figure 3 is also corrected and plotted using the same parameters like in the published version.

Our models still show that structure formation cosmic rays can make a substantial contribution to the extragalactic gamma-ray background, but the data are now more constraining to our models. Resulting contributions are now higher than those derived in some of the papers mentioned in the Discussion and Conclusion section of our published article (Miniati 2002; Colafrancesco & Blasi 1998; Kuo et al. 2005).

## REFERENCES

- Abdo, A. A., Ackermann, M., Ajello, M. et al., 2010, PhRvL, 104, 101101
- Brunetti, G., Blasi, R., Reimer, O. et al., 2012, MNRAS, 426, 956
- Colafrancesco, S., & Blasi, P. 1998, APh, 9, 227
- Fields, B. D., Pavlidou, V., & Prodanović, T. 2010, ApJL, 722, 199
- Kuo, P.-H., Bowyer, S., & Hwang, C.-Y. 2005, ApJ, 618, 675
- Miniati, F. 2002, MNRAS, 337, 199

Pavlidou, V., & Fields, B. D. 2006, *ApJ*, 642, 734

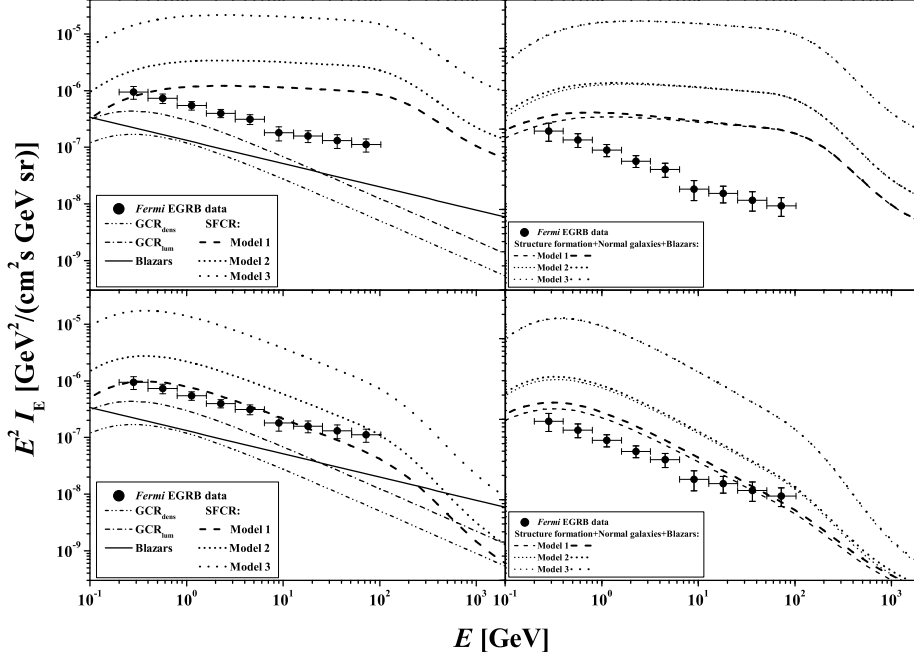


Fig. 4.— Contribution of different components to the extragalactic gamma-ray background (data points) observed by *Fermi* (Abdo et al. 2010). *Left*: all components shown separately – blazars (solid line), normal star-forming galaxies based on two limiting cases given in Fields et al. (2010; red dash dotted line represents luminosity evolution and blue dash dot dotted line represents density evolution), and structure formation cosmic-ray contribution calculated as in the published article, but with the corrected value for  $J_0$ , normalized to the Coma cluster gamma-ray flux limit, with initial gas mass parameter  $\epsilon = 0$ , for three different source models derived in Pavlidou & Fields (2006; long dashed, Model 1; short dashed, Model 2; dotted line, Model 3). Top panel shows structure formation cosmic-ray spectra derived using spectral index  $\alpha_\gamma = 2.1$  and bottom panel  $\alpha_\gamma = 2.7$ . *Right*: the combined contribution of all components where different curves reflect different normal galaxy emission models (thick red curves, luminosity evolution; thin blue curves, density evolution) and different structure formation cosmic-ray emission models (three different line types correspond to the same models as on the top panel). Top panel shows structure formation cosmic-ray spectra derived using spectral index  $\alpha_\gamma = 2.1$  and bottom panel  $\alpha_\gamma = 2.7$ . (A color version of this figure is available in the online journal.)



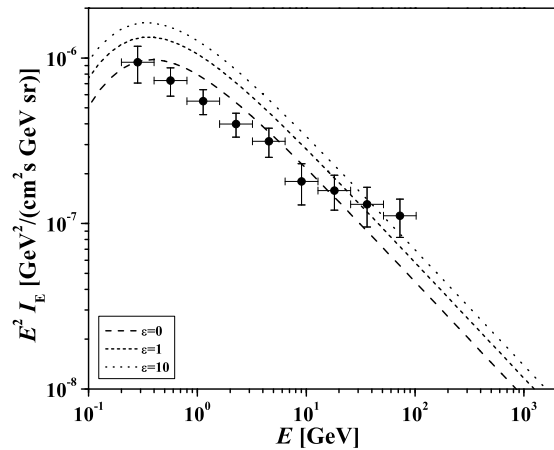


Fig. 5.— This plot shows the sensitivity of our model on the adopted initial gas mass fraction parameter  $\epsilon$ . For the purpose of demonstration, we plot the structure formation cosmic-ray gamma-ray emission for our best-fit model with spectral index  $\alpha_\gamma = 2.7$ , based on Model 1 from Pavlidou & Fields (2006), and derived adopting different initial gas mass fraction values,  $\epsilon = 0, 1, 10$ . The top most curve is approximately a factor of two higher than our best-fit case plotted in Figure 4. For all  $\epsilon > 10$ , all curves converge and are overlapping with the  $\epsilon = 10$  curve.

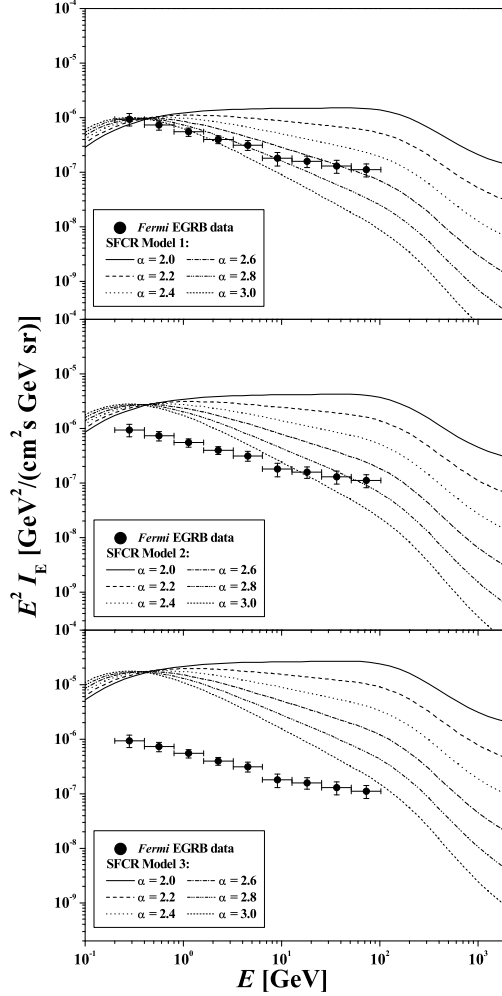


Fig. 6.— Contribution of structure formation cosmic rays to the extragalactic gamma-ray background (data points) observed by *Fermi* (Abdo et al. 2010) for different choices of the cosmic-ray spectral index ranging from  $\alpha_\gamma = 2$  to  $\alpha_\gamma = 3$ , for Model 1 (top panel), Model 2 (middle panel) and Model 3 (bottom panel). The Coma cluster was again taken as the normalizing object with  $\epsilon = 0$ .